Comparing CO_2 retrieved from Atmospheric Infrared Sounder with model predictions: Implications for constraining surface fluxes and lower-to-upper troposphere transport

Yogesh K. Tiwari,[1,2] Manuel Gloor,[1,3,4] Richard J. Engelen,[5] Frederic Chevallier,[6] Christian Rödenbeck,[1] Stefan Körner,[1] Philippe Peylin,[6] Bobby H. Braswell,[7] and Martin Heimann[1]

Received 20 September 2005; revised 29 January 2006; accepted 30 May 2006; published 9 September 2006.

[1] Large-scale carbon sources and sinks can be estimated by combining atmospheric CO_2 concentration data with atmospheric transport inverse modeling. This approach has been limited by sparse spatiotemporal tropospheric sampling. CO_2 estimates from space using observations on recently launched satellites (Atmospheric Infrared Sounder (AIRS)), or platforms to be launched (Infrared Atmospheric Sounding Interferometer (IASI), Orbiting Carbon Observatory (OCO)) have the potential to fill some of these gaps. Here we assess the realism of initial AIRS-based mid-to-upper troposphere CO_2 estimates from European Centre for Medium-Range Weather Forecasts by comparing them with simulations of two transport models (TM3 and Laboratoire Meteorologie Dynamique Zoom (LMDZ)) forced with one data-based set of surface fluxes. The simulations agree closer with one another than with the retrievals. Nevertheless, there is good overall agreement between all estimates of seasonal cycles and north-south gradients within the latitudinal band extending from 30°S to 30°N, but not outside this region. At smaller spatial scales, there is a contrast in the satellite-based retrievals above continents versus above oceans that is absent in the model predictions. Hovmoeller diagrams indicate that in the models, high Northern Hemisphere winter CO_2 concentrations propagate toward the tropical upper troposphere via Northern Hemisphere high latitudes, while in retrievals, elevated winter CO_2 appears instantaneously throughout the Northern Hemisphere. This raises questions about lower-to-upper troposphere transport pathways. Prerequisites for use of retrievals to provide an improved constraint on surface fluxes are therefore further improvements in retrievals and better understanding/validation of lower-to-upper troposphere transport and its modeling. This calls for more independent upper troposphere transport tracer data like SF_6 and CO_2.

Citation: Tiwari, Y. K., M. Gloor, R. J. Engelen, F. Chevallier, C. Rödenbeck, S. Körner, P. Peylin, B. H. Braswell, and M. Heimann (2006), Comparing CO_2 retrieved from Atmospheric Infrared Sounder with model predictions: Implications for constraining surface fluxes and lower-to-upper troposphere transport, *J. Geophys. Res.*, *111*, D17106, doi:10.1029/2005JD006681.

1. Introduction

[2] Atmospheric CO_2 concentration has risen since pre-industrial times from ~280 ppm to ~380 ppm today [*Indermühle et al.*, 1999; *Conway et al.*, 1994], and a halt of the rise is not in sight [*Indermühle et al.*, 1999; *Conway et al.*, 1994]. The principal reason for this trend is increased emissions associated with human activities, such as combustion of fossil fuel, cement manufacture, and land use change [*Keeling et al.*, 1989]. Carbon dioxide is one of the most important and long-lived anthropogenic greenhouse gases, accounting for more than half of human-induced radiative forcing [*Intergovernmental Panel on Climate Change*, 2001]. While much progress in understanding the global carbon cycle has been made, we still lack an adequate understanding of many of the important components of the system. Among them is the nature and

[1] Biogeochemical Systems, Max-Planck Institute for Biogeochemistry, Jena, Germany.
[2] Now at Indian Institute of Tropical Meteorology, Pune, India.
[3] Also at Earth and Biosphere Institute and School of Geography, University of Leeds, UK.
[4] Formerly at Atmospheric and Oceanic Sciences, Princeton University, Princeton, New Jersey, USA.
[5] Satellite Section, Research Department, European Centre for Medium-Range Weather Forecasts, Reading, UK.
[6] Laboratoire des Sciences du Climat et de l'Environnement, Paris, France.
[7] Institute for the Study of Earth Ocean and Space, University of New Hampshire, Durham, New Hampshire, USA.

0148-0227/06/2005JD006681

spatiotemporal distribution of the land carbon sink implied by atmospheric and oceanic carbon inventories [*Sabine et al.*, 2004] when combined with fossil fuel burning emissions [*Marland et al.*, 1985; *Andres et al.*,1996; *Keeling et al.*, 1989; *Tans et al.*, 1990].

[3] One method to estimate carbon sources and sinks is by inverse modeling of atmospheric transport using CO_2 concentration observations [*Rayner et al.*, 1999; *Bousquet et al.*, 2000; *Gurney et al.*, 2002; *Rödenbeck et al.*, 2003]. The method estimates spatiotemporal fluxes by optimizing the mismatch between modeled and observed atmospheric concentrations and the deviation of the flux estimates from prior estimates. These inverse calculations tend to be very sensitive to data uncertainty and model biases, and thus the inclusion of a priori information about fluxes is commonly used to regularize the inversion [*Enting et al.*, 1995]. This Bayesian approach allows simultaneous estimation of an arbitrarily large number of individual fluxes, on the basis of prescribed constraints about spatial and temporal patterns and their covariance structure. All inverse modeling studies published so far are based on observations from a sparse network of near surface atmospheric sampling sites. Furthermore the network is biased toward ocean locations [e.g., *Bakwin et al.*, 1995; *Gloor et al.*, 2000]. The number of surface stations is on the order of 100. In addition, there are continuous records measured on a few tall tower stations, as well as several locations where aircraft are used to measure vertical profiles. Thus, while inversion studies give important insights on the nature of interannual flux variability, the magnitude of the estimates remains of a more qualitative rather than quantitative nature [e.g., *Gloor et al.*, 1999, *Rödenbeck et al.*, 2003], in large part owing to the observational sampling issues discussed above and transport model uncertainties.

[4] Satellite remote sensing of CO_2 permits in principle to sample the atmosphere with much higher density in space and time compared to the current situation. It has thus the potential to reduce strongly the uncertainties of the atmospheric transport inversion approach to estimate carbon sources and sinks. Indeed, several studies that evaluated potential improvements in the results of atmospheric inversion using such data [*Rayner and O'Brien*, 2001; *Houweling et al.*, 2004] confirmed that carbon flux uncertainties would be reduced substantially, assuming unbiased retrievals with normally distributed errors.

[5] *Chedin et al.* [2002, 2003] pioneered the retrieval of CO_2 in the upper troposphere from infrared radiances observed on the NOAA Television and Infrared Observation Satellite Next Generation (TIROS-N) Operational Vertical Sounder (TOVS). The retrievals exhibited qualitatively the expected seasonal cycles and main spatial gradients [*Chedin et al.*, 2003]. In May 2002, the AQUA satellite, which carries the Atmospheric Infrared Sounder (AIRS) instrument, was launched by NASA. Compared to the HIRS-2 (High Resolution Infrared Sounder-2) instrument on TOVS, the AIRS instrument samples the infrared spectral region with a much higher spectral resolution. AIRS covers the 3.7-μm to 15.4-μm region with a spectral resolution of $\lambda/\Delta\lambda = 1200$ [*Aumann et al.*, 2005], recording 2378 channels. In comparison, HIRS-2 measures 20 channels in the 4.3-μm to 15-μm spectral regions, with a spectral resolution between 50 and 100. Taking advantage of these new data, *Crevoisier et al.* [2004] and *Engelen et al.* [2004] and *Engelen and McNally* [2005] have recently developed methods for atmospheric CO_2 retrieval and have begun to estimate atmospheric CO_2 using data from the AIRS instrument.

[6] These recent retrievals using AIRS data should still be viewed as experimental in nature. It is therefore important to confront and analyze these satellite retrievals with our best knowledge and expectations of atmospheric CO_2, before using them to make conclusions about carbon sources and sinks. While the CO_2 distribution at mid-to-upper tropospheric levels (the atmospheric region where AIRS is mainly sensitive to CO_2) is heavily undersampled, at least some insight can be gained from simulation results of the expected signal using atmospheric transport models and "credible" estimates of surface carbon sources and sinks.

[7] The study we present in this paper is dedicated to a comprehensive comparison of the AIRS retrievals of *Engelen and McNally* [2005], with forward model predictions based on the CO_2 flux estimates of *Rödenbeck et al.* [2003] used as boundary conditions in the TM3 and LMDZ models. We will first give the necessary information on the satellite-based retrievals and CO_2 simulations used here, in order to put the results of the comparisons into perspective. Next, we will discuss in a zonal mean context the upper troposphere CO_2 signal that is expected from a modeling perspective, given our best knowledge of surface processes and atmospheric transport. An analysis of similarities and differences between retrievals and simulation predictions will then be presented, starting from spatially and temporally averaged quantities, and proceeding gradually from coarser to finer-scale spatial features. We will then summarize and discuss the value of the AIRS data to constrain analyses of carbon cycling and tropospheric transport.

2. Methods

2.1. AIRS CO_2

2.1.1. Retrieval Approach

[8] AIRS CO_2 retrievals for the year 2003 used in this study were obtained with a column estimation method that was implemented in the ECMWF 4D-Var data assimilation system by *Engelen et al.* [2004] and *Engelen and McNally* [2005]. The main principle employed is that radiances in the thermal infrared region (3.7–15.4 μm) are sensitive to both temperature and, to a lesser extent, the concentration of CO_2. If temperature profiles can be estimated with high accuracy, then the remaining difference between predicted and observed radiances can be attributed to CO_2 (assuming perfect spectroscopy and radiative transfer modeling) [e.g., *Chedin et al.*, 2003; *Crevoisier et al.*, 2003]. More formally, the relation between the radiance observed by the satellite,

$$I_\nu = F_{\mathrm{mod}\,el,\nu}(CO_2, \alpha) + \varepsilon_{meas}, \quad (1)$$

at a set of frequencies ν, which are selected optimally with respect to signal to noise, is inverted within the framework of the ECMWF 4D-Var data assimilation system. Here CO_2 stands for the CO_2 profile along the line of sight of the satellite instrument, α represents the remaining parameters that characterize the thermodynamic state and atmospheric condition of the profile, and ε_{meas} is the measurement error.

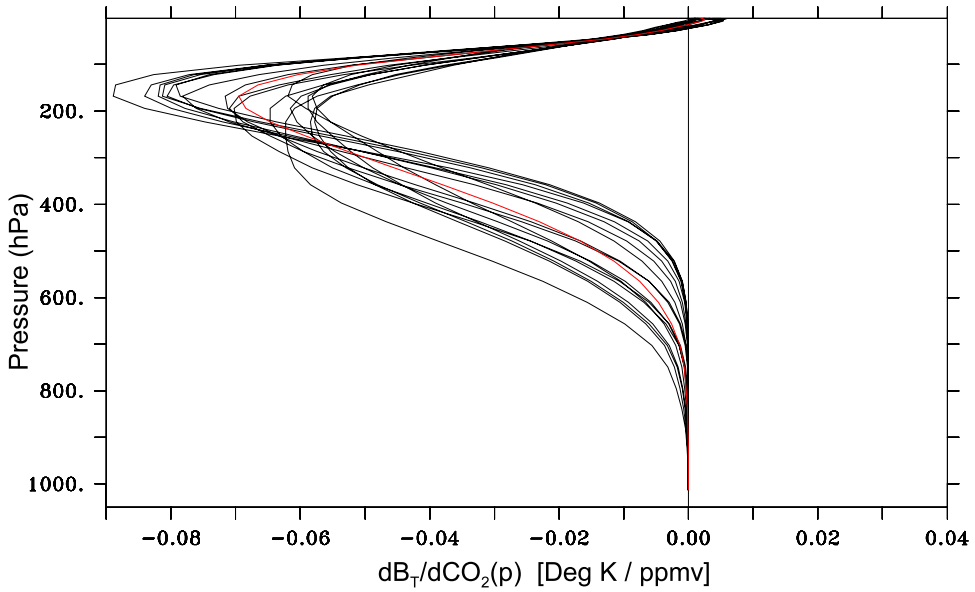

Figure 1. Weighting function for the 18 channels (black) used to retrieve CO_2 from AIRS data within the ECMWF weather forecast model, and the mean weighting function (red) used for weighting model concentrations for comparison with AIRS retrievals.

The function F is approximated by the solution of the radiative transfer equation for a nonscattering plane-parallel atmosphere in local thermodynamic equilibrium, and is a nonlinear function of the CO_2 profile [see *Engelen and McNally*, 2005]. Because inversion of equation (1) is an ill-posed problem, the following functional,

$$J = (I - F_{\mathrm{mod}\,el})^t S_{meas}^{-1} (I - F_{\mathrm{mod}\,el}) + \left(CO_{2,prior} - CO_2\right)^t S_{prior}^{-1} \cdot \left(CO_{2,prior} - CO_2\right), \quad (2)$$

is minimized instead. Here $CO_{2,\mathrm{prior}}$ is an a priori prescribed CO_2 profile and S_{meas} and S_{prior} are the error covariance matrices of the measurements and of the a priori CO_2 profile, respectively. The other relevant parameters in the radiative transfer equation (temperature, water vapor, and ozone) are initially provided by the model forecast and are adjusted within the assimilation at the same time as CO_2, using various sources of observations. All observations are bias corrected to fulfill the requirement of unbiased statistics. The bias correction used by ECMWF is based on 1 month of radiance model prediction versus observation comparisons. The retrieval results presented here are based on a temporally and spatially uniform prior CO_2 distribution, and with prior estimate of 376 ppm and prior uncertainty 30 ppm. Instrument and observation errors are assumed to be uncorrelated and to be 0.6 K. Eighteen channels were selected that are sensitive almost exclusively to mid and upper tropospheric CO_2. The vertical distribution of the sensitivity of the radiances to CO_2, measured at the 18 frequencies, is given in Figure 1 (reproduced from work of *Engelen and McNally* [2005]).

2.1.2. AIRS Characteristics and Spatiotemporal Retrieval Coverage

[9] AIRS was launched into a 705-km-altitude polar orbit on the EOS Aqua aircraft on 4 May 2002, and has an expected on-orbit lifetime of 7 years. The instrument field of view is 1.1°, corresponding to a nadir footprint of 13.5 km on the surface. The scan angles vary from 49°S to 49°N

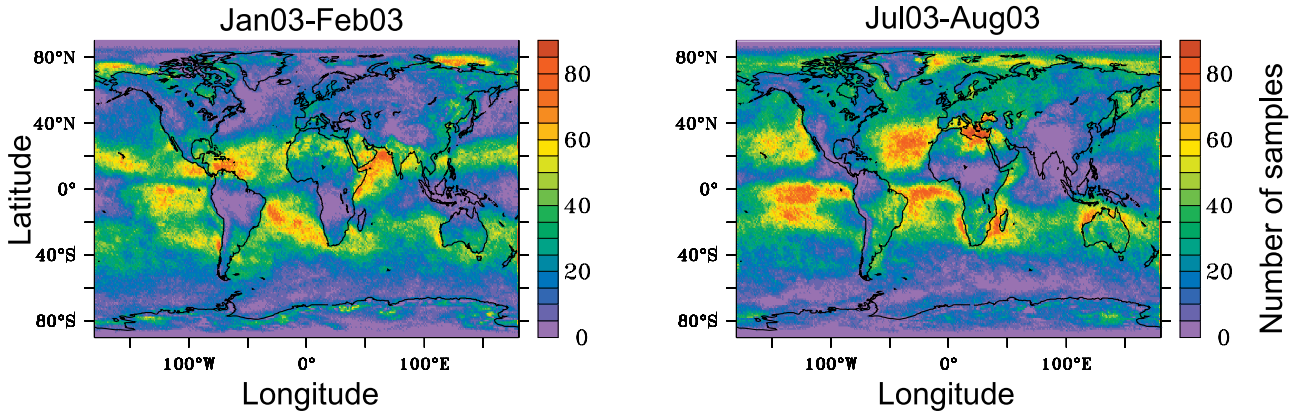

Figure 2a. Number of AIRS retrievals per 1° × 1° grid box for two 2-month periods.

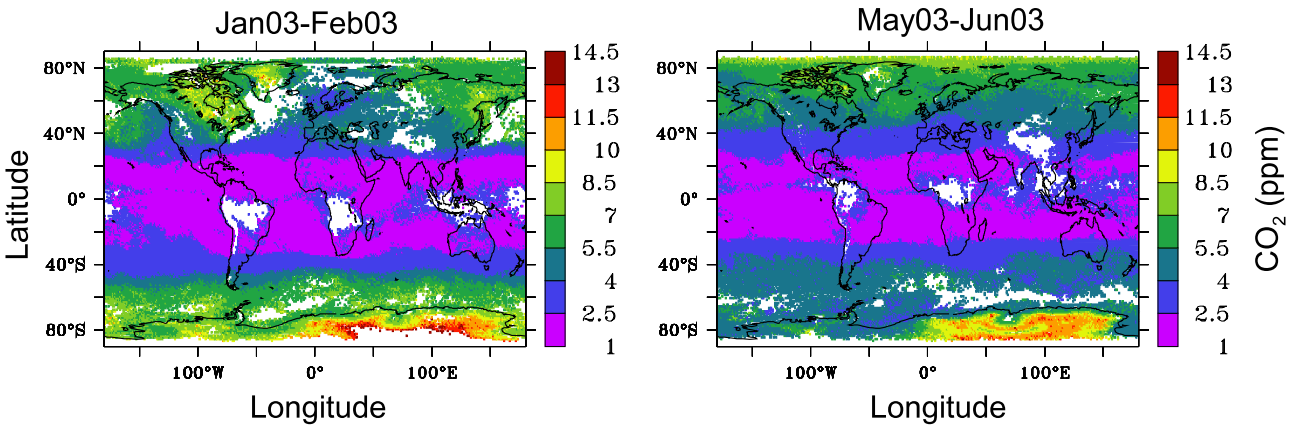

Figure 2b. AIRS retrieval average error per 1° × 1° grid box for two 2-month periods.

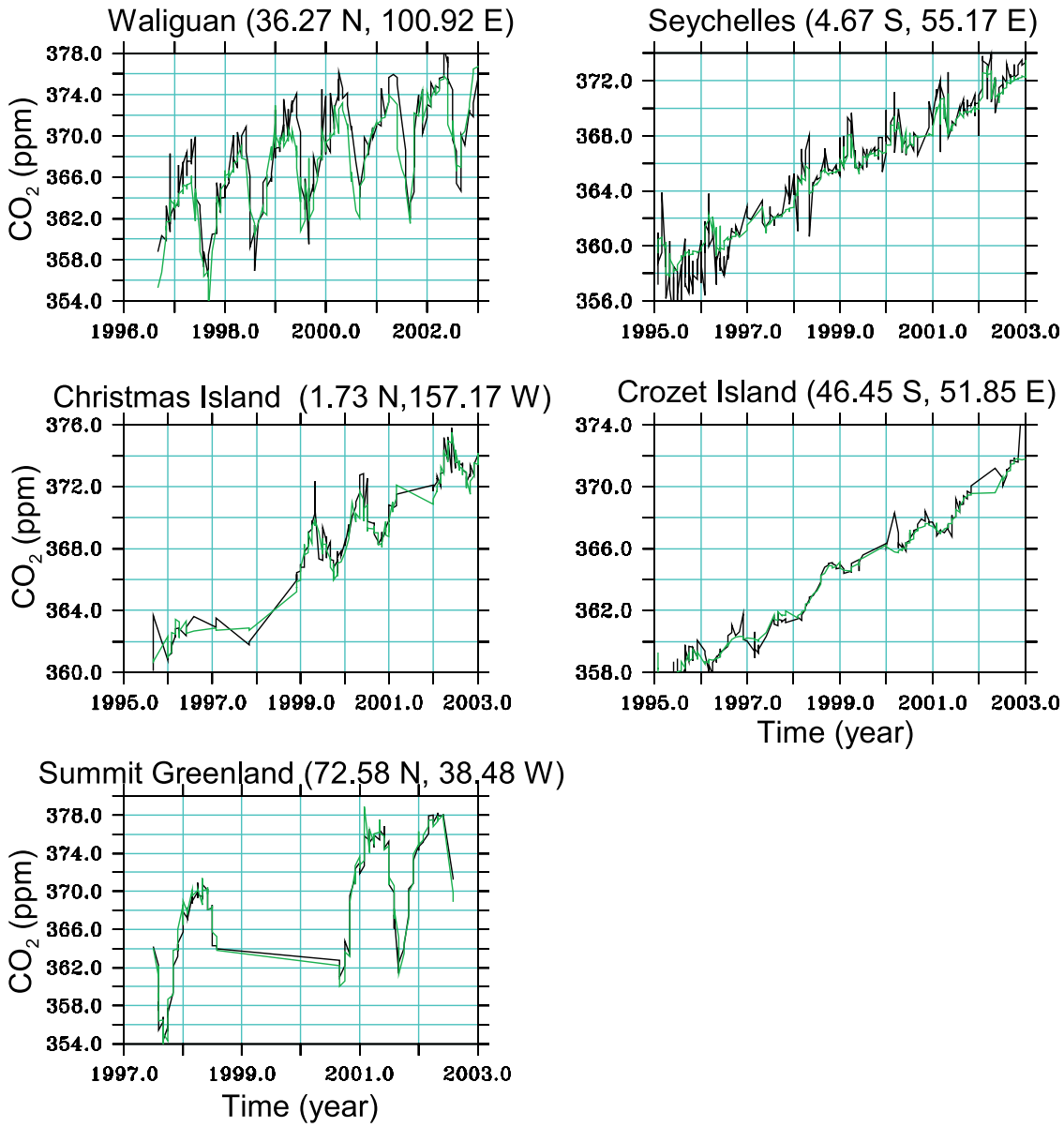

Figure 2c. Comparison of TM3 simulated CO_2 (ppm) mixing ratio with surface CO_2 (ppm) observations from NOAA/CMDL. Surface observation records (black lines) have not been used to estimate fluxes which are used to simulate model.

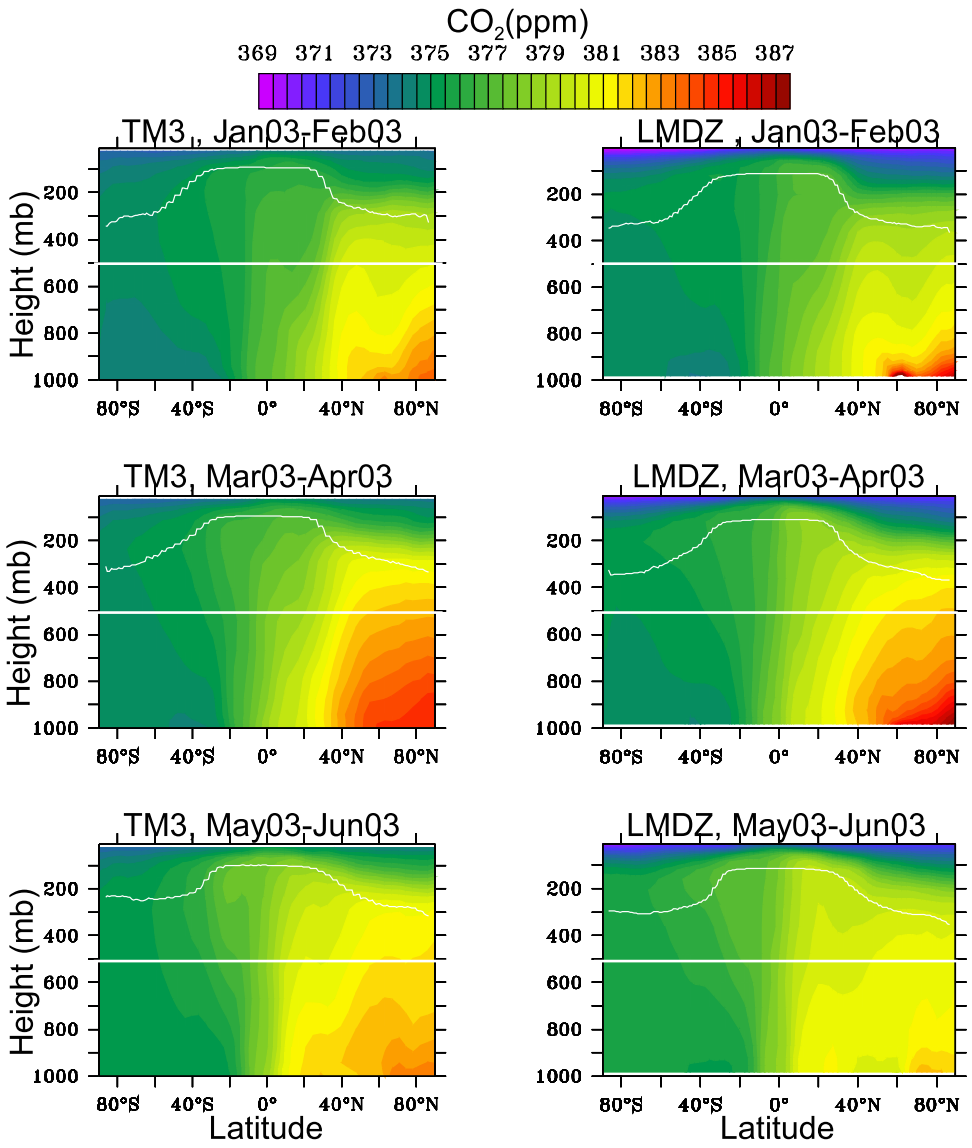

Figure 3a. Vertical distribution of CO_2 mixing ratio at 170° West, during the first half of the year 2003, as simulated by (left) TM3 and (right) LMDZ. The upper white lines delineate the tropopause height; the lower lines delineate the lower boundary of the troposphere region to which AIRS CO_2 retrievals are mainly sensitive.

[*Aumann et al.*, 2003]. The satellite crosses the equator at approximately 1:30 am and 1:30 pm, resulting in global coverage twice a day. Most clouds are opaque at the radiance frequencies used in the CO_2 estimation. In order not to lose all information about the atmospheric profile in the presence of clouds, *McNally and Watts* [2003] developed a cloud detection scheme that identifies which channels are not affected by clouds. Within the ECMWF data assimilation system, this scheme identifies and removes those AIRS channels that are affected by clouds, and keeps only those channels which are cloud free. CO_2 estimates were only used when all 18 AIRS CO_2 channels were not affected by clouds. The typical number of uncontaminated data samples observed by AIRS is displayed in Figure 2a. These sampling frequencies range from 10 to 90 per $1° \times 1°$ grid box per month. As expected, the coverage is large in subsidence regions (~50 profiles per month) but very low in the ITCZ region (0–10 profiles per month). The figures indicate that month to month variability of data coverage is low.

2.2. Model Predictions of Atmospheric CO_2

[10] Atmospheric CO_2 is predicted in this study by applying CO_2 fluxes estimated by *Rödenbeck et al.* [2003] as boundary conditions in the atmospheric transport models TM3 [*Heimann and Körner*, 2003] and LMDZ [*Sadourny and Laval*, 1984; *Hourdin and Armengaud*, 1999]. Using a similar method as described by *Rödenbeck et al.* [2003] and using atmospheric CO_2 concentration data based on 39 surface stations the fluxes cover the period of 1996 to 2003 with approximately weekly temporal resolution [*Rödenbeck*, 2005]. Both model simulations start in January 2000 and end in December 2003. For the comparisons, the last year of the simulations (year 2003) is used. A limited

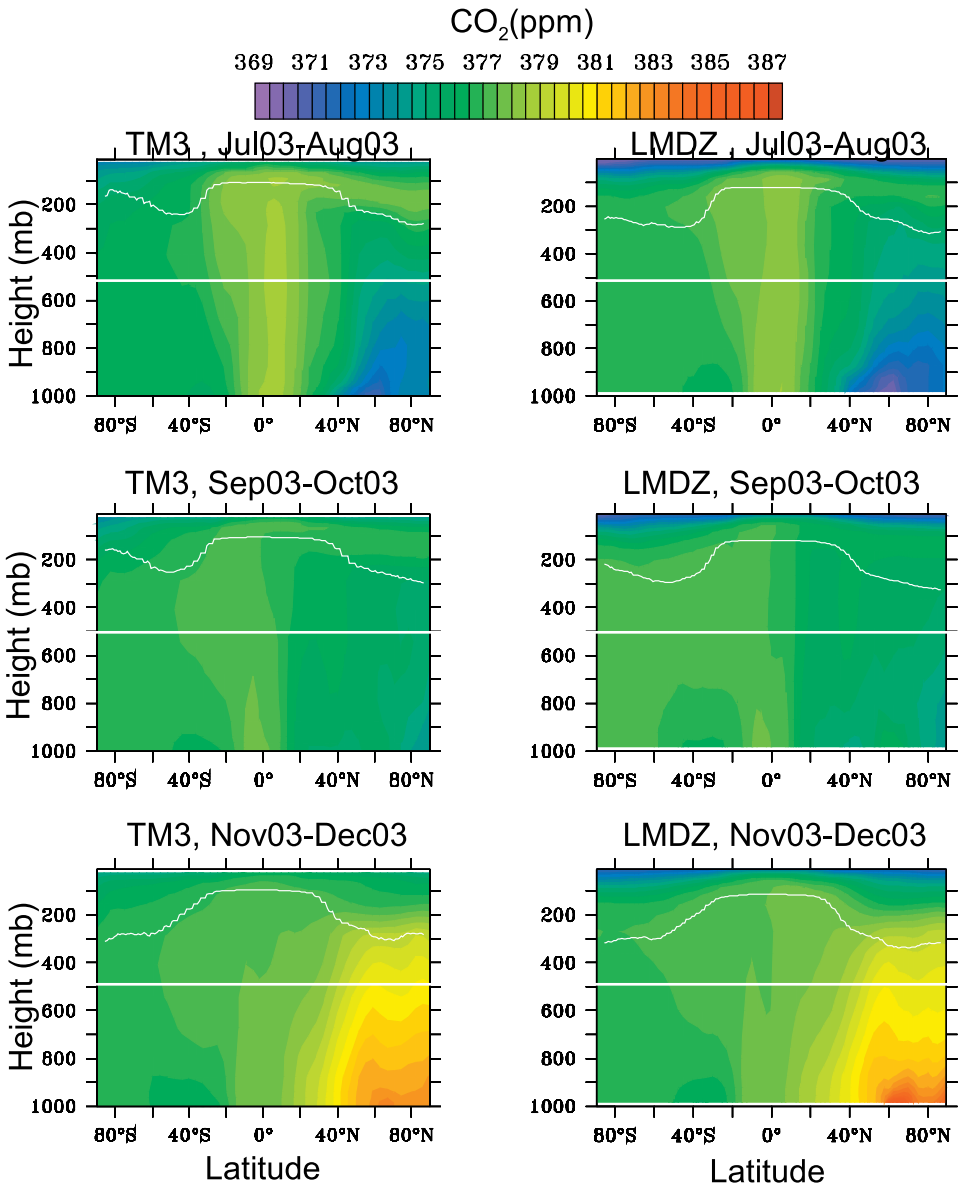

Figure 3b. Same as Figure 3a, but for second half of year 2003.

assessment of the realism of these fluxes is provided by a comparison of the concentration predictions at stations not used for the inversions to estimate surface fluxes (Figure 2c). These station records have been excluded deliberately from the inverse calculations because of concerns of data quality, limited temporal coverage or representability of the station in models with the model resolution employed in this study. The fairly good agreement indicates that the surface flux estimates are quite realistic but that there are limitations particularly at high altitude stations like Waliguan (WLG). Reasons for differences may be related to measurement problems and representation problems of the stations, however a detailed analysis is out of scope of this paper.

2.2.1. Atmospheric Transport Models

[11] Both atmospheric transport models employed in this study solve the continuity equation for an arbitrary number of atmospheric tracers on a regular grid spanning the entire globe. The horizontal resolution of the TM3 model is 4° × 5° latitude by longitude with 19 sigma-coordinate layers in the vertical. Transport in TM3 is driven by meteorological fields derived from NCEP (National Center for Environmental Prediction) reanalysis [*Kalnay et al.*, 1996]. Tracer advection is calculated using the slopes scheme of *Russell and Lerner* [1981]. Vertical transport due to convective clouds is computed using the cloud mass flux scheme of *Tiedtke* [1989], and turbulent vertical transport is computed using the stability dependent vertical diffusion scheme of *Louis* [1979]. TM3 requires, as input, global fields of vertical diffusion coefficients and cumulus cloud transport fields. The cloud transport fields consist of entrainment and detrainment rates in updraft and downdraft, as well as updraft and downdraft mass fluxes. These are calculated in the preprocessing stage from meteorological analyses of geopotential height, surface pressure, horizontal wind, temperature, and specific humidity. Finally, surface fluxes of latent heat are used [*Heimann and Körner*, 2003] by TM3.

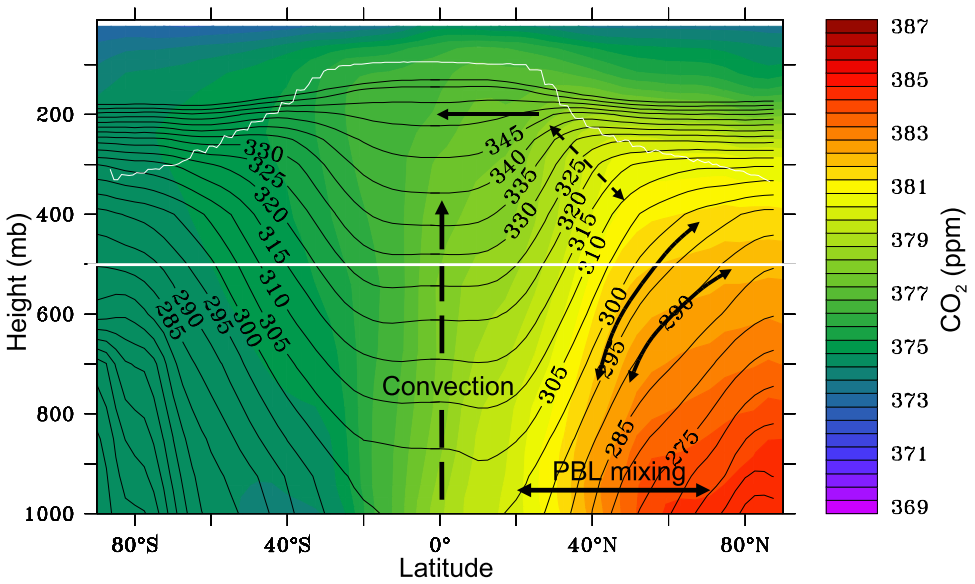

Figure 4. Zonally averaged monthly mean potential temperature (°K) plotted over zonally averaged monthly mean TM3 simulated CO_2 (ppm) mixing ratio for March and April 2003. Solid black arrows indicate mixing along the isentropes, and dashed arrows indicate mixing across isentropes. The tropopause is marked by a curved white line, and lower boundary of AIRS weighting function is marked by a solid straight white line.

[12] The second atmospheric tracer transport model used in this study is the LMDZ general circulation model (GCM), which is used here with a horizontal resolution of 2.5° × 3.75° latitude by longitude and 19 sigma coordinate layers in the vertical. The model solves the full dynamic equations for winds. The model-calculated winds are then relaxed toward ECMWF analyzed meteorology with a relaxation time of 2.5 hours, in order to force transport to reproduce the observed large scale advection [*Bousquet et al.*, 2005]. The model uses the advection scheme of *Hourdin and Armengaud* [1999]. Deep convection is parameterized using the *Tiedtke* [1989] scheme, and turbulent mixing in the boundary layer is based on work by *Laval et al.* [1981]. The main differences between the two models are first the

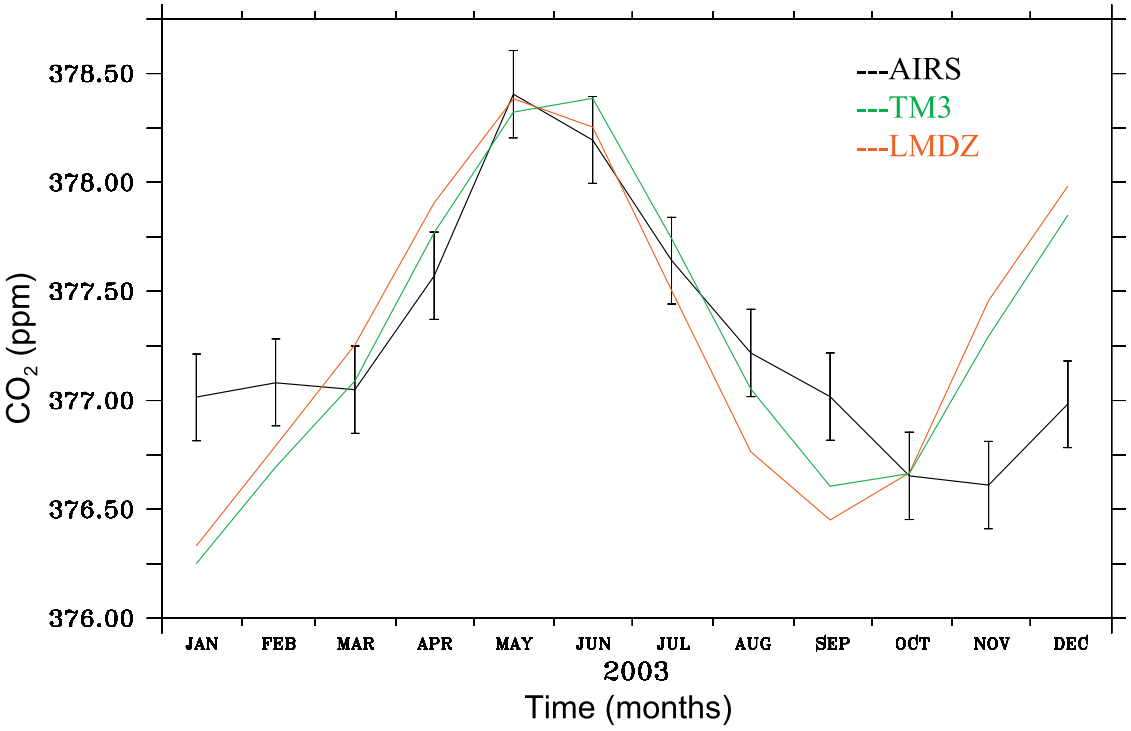

Figure 5. Zonally averaged CO_2 between 60°S and 60°N, as retrieved by AIRS and simulated by TM3 and LMDZ.

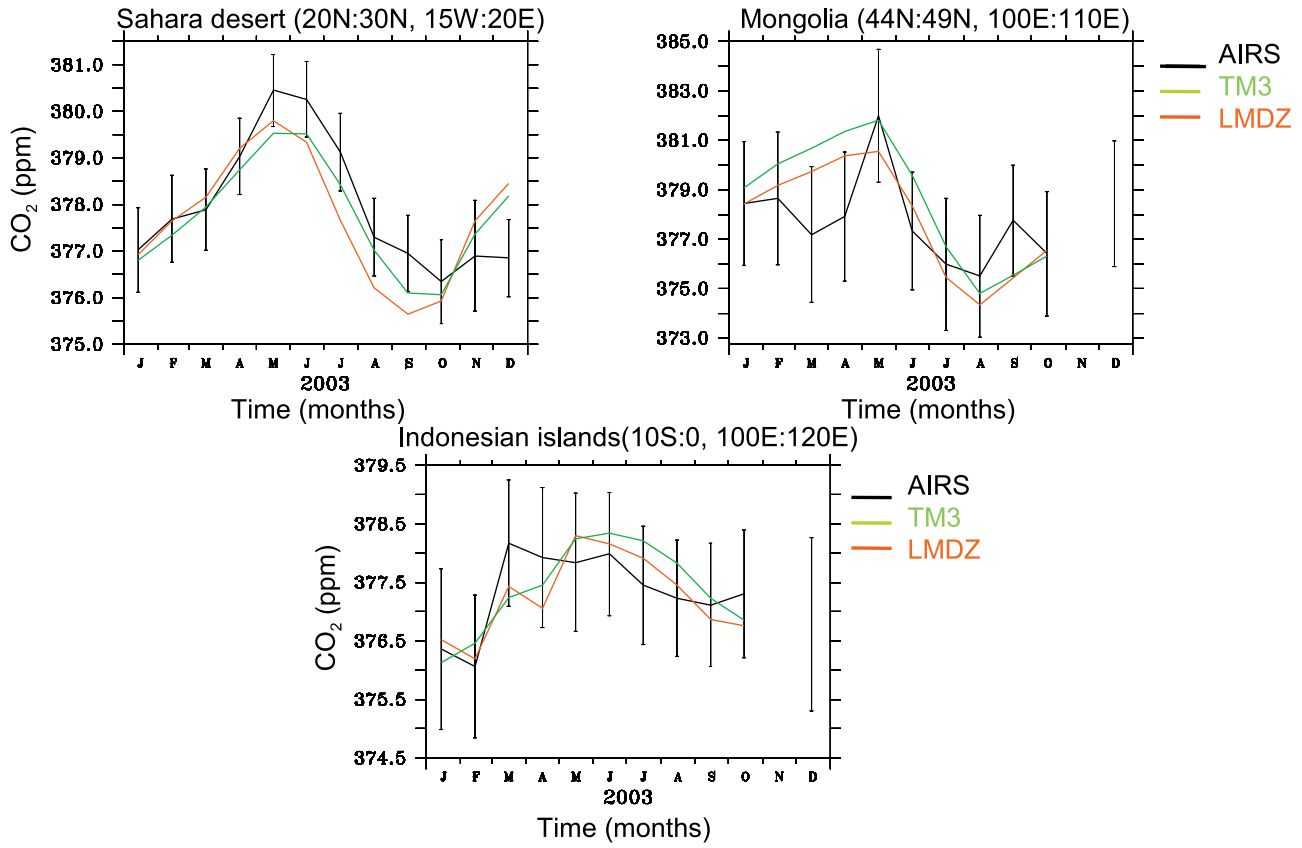

Figure 6. Regionally averaged CO_2, as retrieved by AIRS and simulated by TM3 and LMDZ for three selected regions.

spatial resolution, with TM3 having a coarser resolution than the LMDZ model. Second, the LMDZ model is a full GCM that is used in a nudging mode, whereas TM3 is an off-line model which uses analyzed winds for time stepping the discretized transport equation. Third, the meteorological fields used to solve model transport equation differ. The sub-grid-scale parameterizations of the two models are rather similar.

2.2.2. Surface Fluxes

[13] Using essentially the same method as described by *Rödenbeck et al.* [2003] the CO_2 surface fluxes of the atmospheric transport inversion study by *Rödenbeck* [2005] vary approximately weekly and cover the period from 1996 to 2003; they are based on near-surface CO_2 concentration data from 39 stations of the NOAA/CMDL network (update of *Conway et al.* [1994]). The inverse calculations are based on the TM3 model, and have been regularized assuming exponentially decaying spatial a priori correlations of the fluxes, in concert with prescribed prior fluxes in a Bayesian framework. The spatial resolution of the fluxes is $8^\circ \times 10^\circ$ latitude by longitude. More detailed information is available in the original manuscripts by *Rödenbeck et al.* [2003] and *Rödenbeck* [2005].

2.3. Specifics of Model Sampling for Retrieval Model Simulation Comparison

[14] For all comparisons, we restricted ourselves to the latitude band between 60°N and 60°S, because the AIRS retrieval error estimates become very large at high latitudes (Figure 2b), and thus the retrievals are of limited use for constraining carbon sources and sinks at the surface. AIRS retrieval average errors in Figure 2b were calculated taking spatial and temporal error correlations into account following *Engelen and McNally* [2005]. To perform a proper comparison between the retrievals and the model simulations, the simulations are sampled at the same locations and same times as the retrievals. For each AIRS column observation, the model is sampled below the tropopause height only. This is because AIRS retrievals are based on weighting functions modified to be zero above the tropopause [*Engelen and McNally*, 2005]. Tropopause height is estimated using the algorithm employed by ECMWF, which is based on the WMO (1957) lapse-rate criterion as implemented by *Reichler et al.* [2003]. The samples are then weighted with the mean weighting function in Figure 1. The simulations permit comparison only up to a constant offset. The offset we added to the simulations is the difference between the annual mean AIRS signal and the annual mean weighted CO_2 simulation results, covering the 60°S to 60°N region of the globe.

3. Comparison of AIRS Retrievals With Model Simulations

3.1. Expected Signals and Conceptualization of Model Lower-to-Upper Troposphere Transport

[15] The upper troposphere region (where AIRS is sensitive to CO_2) is only indirectly related to surface fluxes via

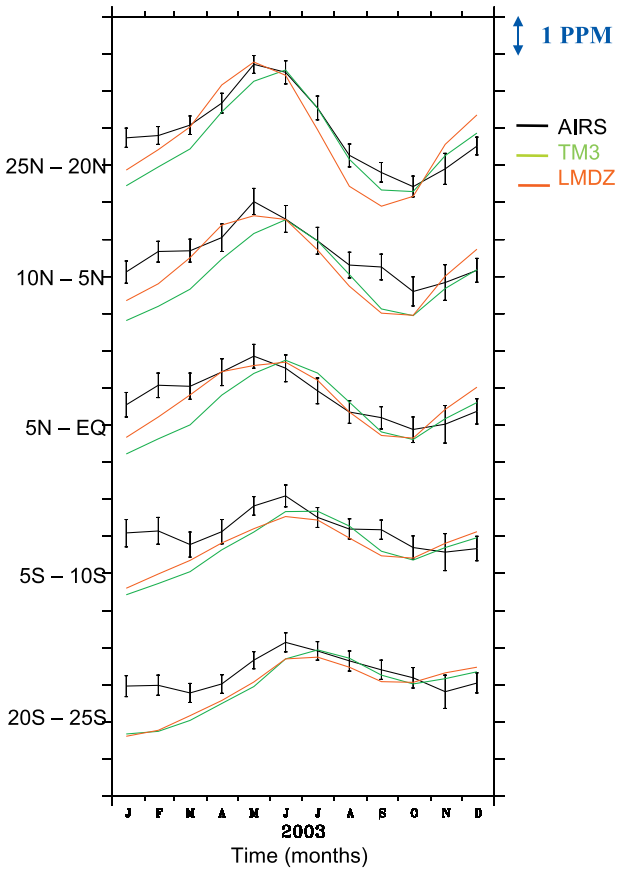

Figure 7. Monthly mean CO_2 (ppm), averaged zonally and over 5° latitudinal bands, as retrieved by AIRS and simulated by TM3 and LMDZ.

lower troposphere transport, and thus the effect of surface fluxes on concentrations in this region is not entirely obvious. To gain intuition about the nature of signals that are likely to be seen by AIRS, and which transport routes are responsible, it is therefore instructive to consider model predictions. Specifically, we analyzed the latitude-height sections of atmospheric CO_2 for the four seasons (Figures 3a and 3b), using both the TM3 and the LMDZ model. Similar to the situation near the Earth's surface, upper troposphere CO_2 is dominated by the interplay between fossil fuel emissions, located mainly in the Northern Hemisphere midlatitudes, and the seasonal cycle of carbon release and uptake by the land vegetation in the Northern Hemisphere. As a result, Northern Hemisphere upper troposphere concentrations exhibit a clear seasonal cycle that weakens toward the tropics and is largely absent in the Southern Hemisphere. Compared to the lower troposphere, signals are generally weaker and somewhat lagged, and the regions where N-S gradients are largest are shifted latitudinally compared to the surface region. In the upper troposphere, the largest gradients occur around 30°N and 30°S (this is particularly visible in the top two panels of Figures 3a and 3b), while in the lower troposphere gradients are located more to the north to about 50°N. The shift of regions with the largest gradients is a reflection of the effect of tropospheric transport on surface concentrations.

[16] A tentative conceptual view of pathways from the surface to the upper troposphere in the Northern Hemisphere region is overlaid on top of isentropes (surfaces of constant potential temperature) calculated from the 2003 NCEP reanalysis (NCEP/NCAR reanalysis data provided at http://www.cdc.noaa.gov/) and atmospheric CO_2 simulated with TM3 (Figure 4). In these models, CO_2 isosurfaces tend to be aligned outside the tropics with constant potential temperature surfaces. This is a reflection that air parcel motion in the mid-to-high latitude free troposphere is, to first order, adiabatic. Equivalently, this indicates that tracer dispersion along isentropic surfaces is much faster than across isentropic surfaces. Largest concentration gradients in the upper troposphere indeed occur where the potential temperature surface curve the strongest; presumably this is related to the "potential vorticity barrier" located there [*Mahlman*, 1997].

[17] A characteristic of the troposphere that is important for transport to the tropical upper troposphere is that potential temperature surfaces in the Northern Hemisphere midlatitudes slope differently in the lower troposphere compared to the upper troposphere. As a consequence, one pathway for Northern Hemisphere midlatitude air, laden with fossil fuel CO_2, to pass to the upper tropical troposphere is via the northern mid-to-high latitudes. Lower troposphere air is dispersed toward the midtroposphere mainly along upward sloping constant potential temperature surfaces and to a lesser degree across isentropes. In the jet stream regions, air masses are mixed across isentropes (and across potential vorticity gradient) by breaking tropospheric cyclone waves into the tropical upper troposphere [*Mahlman*, 1997].

[18] An alternative pathway is the dispersal of CO_2 laden air in the Planetary Boundary Layer (PBL) toward the tropics, and subsequent transport to the upper tropical troposphere via deep convection. To obtain a measure of the roles played by parameterized tropical convection for lower troposphere–upper troposphere CO_2 transport we have repeated all the model simulations but with parameterized convective transport turned off. Surprisingly the lack of parameterized tropical convection did not change the CO_2 signatures in the upper troposphere to a great extent indicating that the pathway via Northern Hemisphere mid-to-high latitudes may be most important for lower-to-upper troposphere tracer transport from midlatitudes.

[19] In summary, from simulations we expect similar seasonality in upper troposphere CO_2 as is observed near the ground, but of a lower magnitude and with time delays compared to the timing of surface fluxes on the order of 1 month. We also expect the largest concentration gradients around 30°N, on the basis of the atmospheric potential temperature distribution and the differences in simulated upper tropospheric CO_2. However, this result depends upon the relative roles of the two transport branches sketched above.

3.2. Comparisons

3.2.1. Temporal Structure

[20] The lowest order diagnostic, the spatially averaged CO_2 distribution (Figure 5), reveals overall a qualitatively good agreement between retrievals and models. The amplitude of the seasonal variation of the signals is very similar.

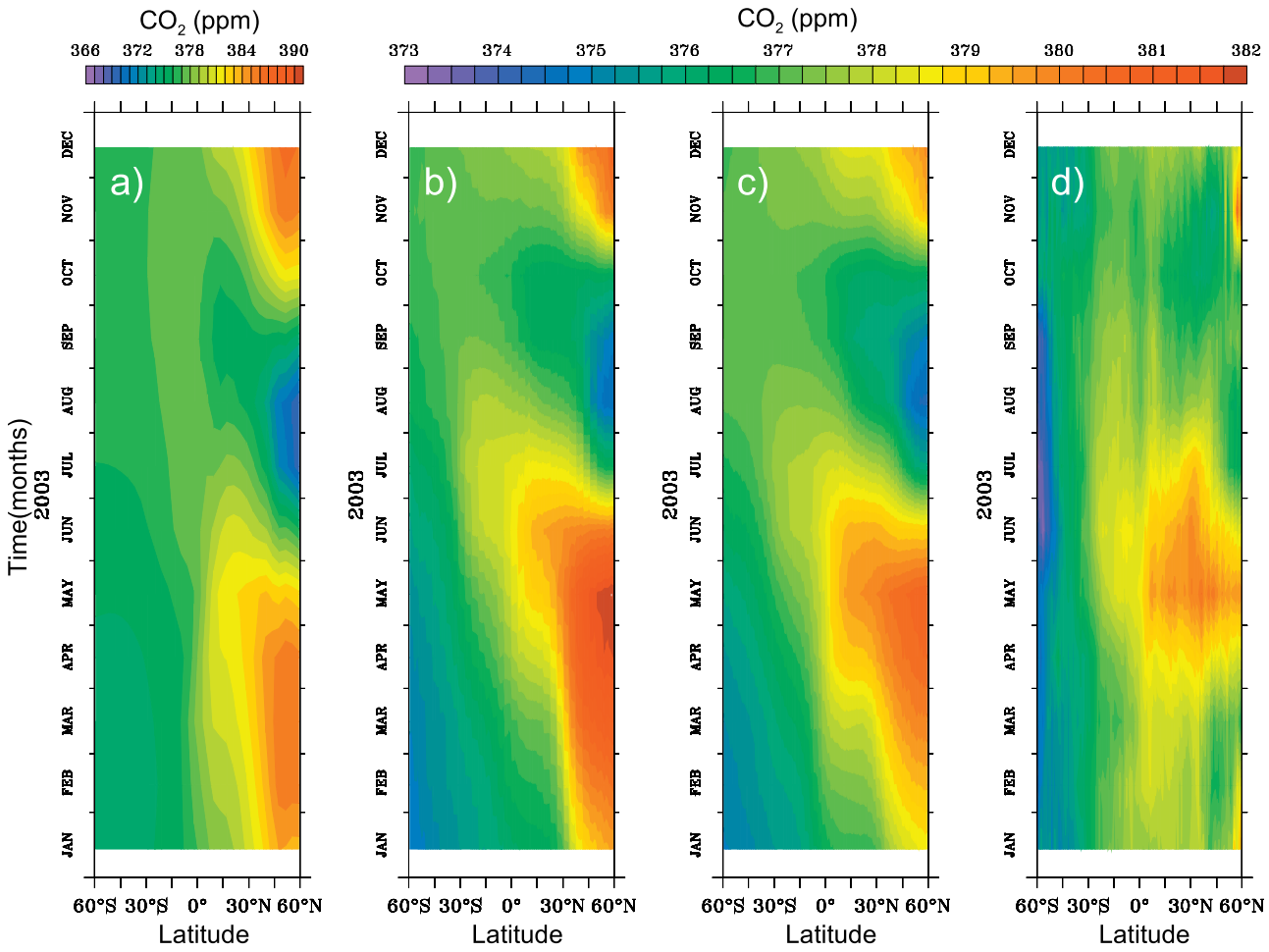

Figure 8. Zonal mean CO_2 (ppm) versus time for the year 2003. (a) TM3 simulated surface CO_2 (ppm) mixing ratio, (b) TM3 weighted column CO_2 (ppm), (c) LMDZ weighted column CO_2 (ppm), and (d) AIRS retrievals weighted column CO_2 (ppm).

There is a difference in the timing of the increase of carbon dioxide just after the phase of decrease due to summer drawdown, caused by photosynthesis on land. This may be an indication that the models exaggerate the upward propagation of surface signatures during late summer and autumn. Alternatively, surface fluxes may be biased in time, or there may be a bias in the retrievals. One element that is absent in the AIRS retrievals is the trend caused by continuous burning of fossil fuels. Atmospheric surface concentration records from CMDL show that the growth of atmospheric CO_2 in 2003 was not unusually low. Furthermore, the observed stratospheric CO_2 growth rate generally follows closely the observed growth rate at the earth surface [*Boering et al.*, 1996]. Therefore atmospheric data seem to support the model simulations rather than the retrievals in this regard. It is interesting to note that the AIRS retrievals sampled at the location of high altitude stations like Hawaii do exhibit a similar trend recorded by the high-altitude station itself [*Engelen and McNally*, 2005]. This indicates that the averaging procedure may hide some of the trend information contained in the retrievals.

[21] In order to visualize the degree of agreement and disagreement on a finer, but still somewhat coarse, spatial scale, the monthly mean time series for a few randomly selected regions covered mostly by land are displayed in Figure 6. For the Sahara and Indonesia regions, the agreement is again surprisingly good, while it is worse for the Mongolia region. For the Sahara region, there is again somewhat of a delay in the phases of increase and decrease associated with the upward propagating seasonal surface signal, compared to simulations. The AIRS-based signal over Mongolia is less smooth and its seasonality is less expressed. The reason for the disagreement is not clear. Generally, model simulations are closer to one another than to AIRS retrievals.

[22] Next, we compared zonal mean seasonal signals averaged over 5° latitude bands (Figure 7). Amplitudes of the seasonal signal, and its decrease with decreasing latitude, agree well between AIRS retrievals and model simulations. The amplitude of the retrievals tends to be slightly smaller, particularly in the tropics and Southern Hemisphere. There are, however, some differences in the phasing of the seasonal signals. The onset of the summer drawdown signal simulated by LMDZ in the Northern Hemisphere, between the equator and 25°N, precedes the retrievals by approximately 1 month. These, in turn, precede the TM3 simulations by 1 month. The reason for the different phasing between the models is likely due to differences in

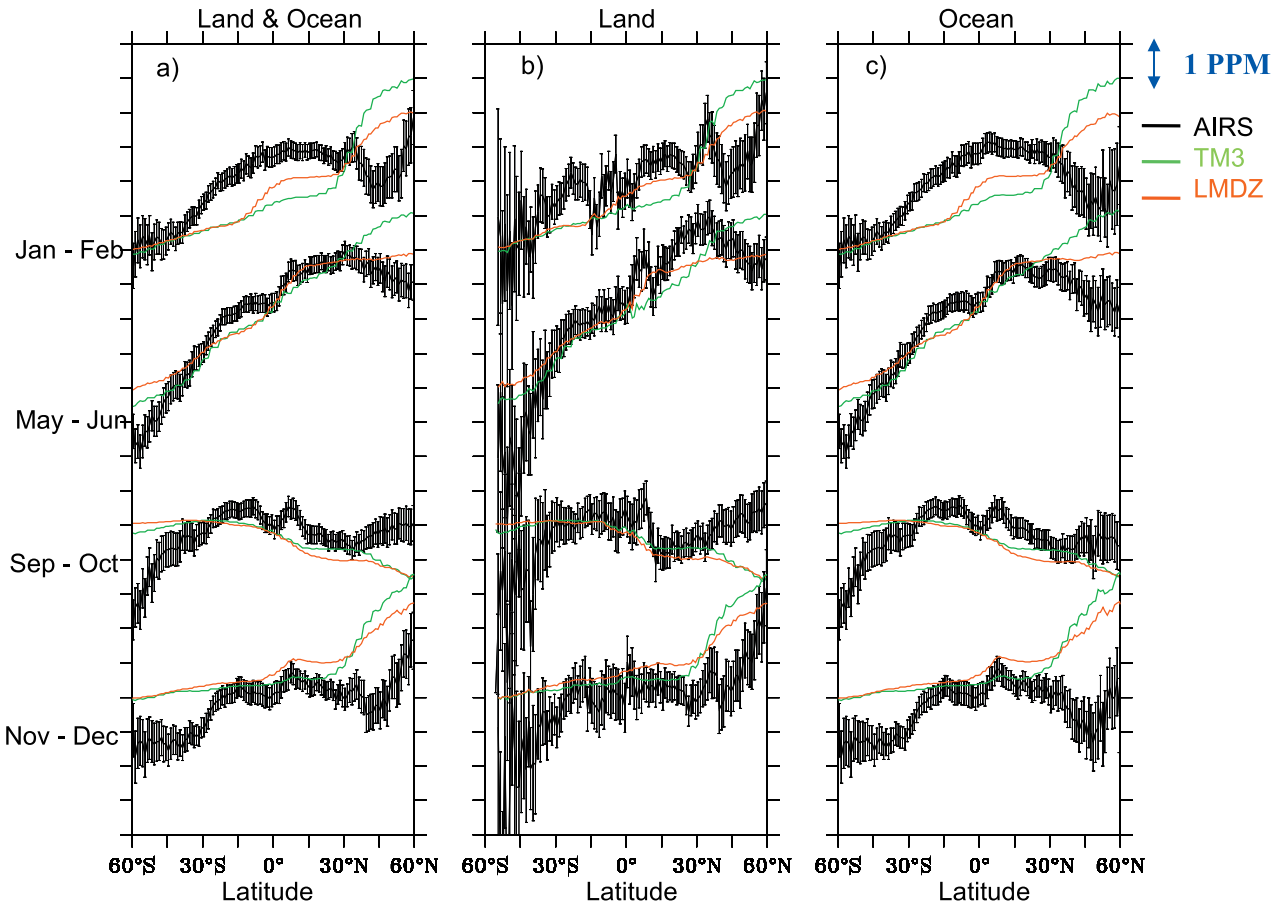

Figure 9. Zonal mean latitudinal variation of CO_2 (ppm) averaged over two months. (a) over land and ocean, (b) only over land, and (c) only over oceans.

lower-to-upper troposphere transport. In particular, LMDZ may communicate surface fluxes too fast to the upper troposphere, while TM3 may be too slow. A possible explanation for model differences may be differences in across-isentropical mixing, due to differences in the meteorological fields (NCEP versus ECMWF). A related but somewhat different reason may be that the LMDZ model is a full GCM used in a data assimilation mode, while TM3 uses NCEP meteorological fields directly (i.e., without modifications). The point at which CO_2 begins to increase again in autumn agrees well between all estimates in the zone from the equator to 25°N, but retrievals lag both simulations by approximately 2–3 months in the tropics and in the Southern Hemisphere. It could be an indication of misrepresentation of transport in the models. A lag is expected if the pathway of the Northern Hemisphere fossil fuel burning signal toward the tropics is via high latitudes, and subsequently the upper troposphere. On the other hand, if the Northern Hemisphere fossil fuel burning signal is dispersed latitudinally by mixing in the planetary boundary layer first and then communicated to the upper troposphere by convection, the lag is likely to be smaller. It is interesting to note here that over the western Pacific the AIRS retrievals compare very well in terms of amplitude and phase with in situ flight observations [*Engelen and McNally*, 2005]. A similar picture emerges when comparing zonal mean fields as a function of time (Figure 8). While there is a clear N-S propagation of the Northern Hemisphere spring maximum CO_2 signal discernible in the TM3 and LMDZ simulations, due to fossil fuel burning and the absence of photosynthesis on land in the winter, the AIRS retrievals reveal a maximum signal that occurs almost instantaneously over the entire latitude range (60°S–60°N). Further analysis of the AIRS estimates indicates that there is a potential for bias outside the tropical area. Depending on the difference between real stratospheric CO_2 values and stratospheric values used in the assimilation radiative transfer model, a bias of up to 2 ppmv can end up in the estimates. This suggests that the use of AIRS estimates outside the tropics likely has to be limited. An alternative explanation is that, in these models, the pathway of Northern Hemisphere midlatitude fossil fuel burning CO_2 to the upper tropical troposphere is biased toward the high latitude pathway at the cost of the convection mid- and low-latitude pathway.

3.2.2. Spatial Gradients and Patterns

[23] As will be evident from the comparison of the 2-D spatial patterns, there is a land-sea contrast in the AIRS signals. We therefore consider not only the global zonal mean gradients but also separately the mean gradients for land and ocean regions (Figure 9). Generally, as in the previous comparisons, the intermodel agreement is better than the agreement between the simulations and the AIRS

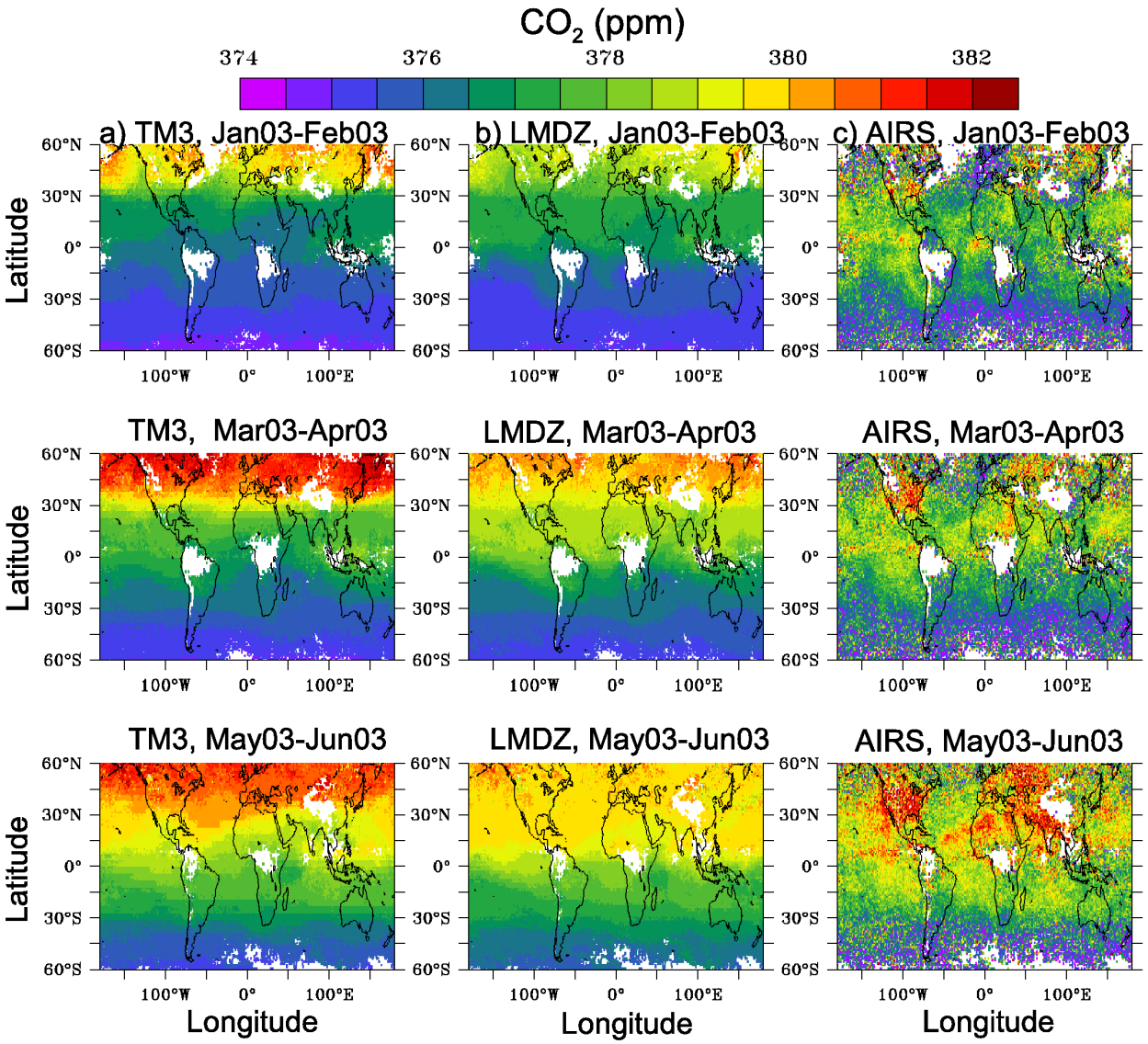

Figure 10a. Two monthly mean maps of upper tropospheric CO_2, as simulated by (column a) TM3, (column b) LMDZ, and (column c) retrieved by AIRS.

retrievals. Also, differences between model predictions and retrievals are generally larger outside the tropical region extending approximately from 30°S to 30°N possibly because of the increase in retrieval biases outside the tropics mentioned earlier on. Looking into greater detail, there is quite good agreement in the latitudinal gradients during summer and autumn, but there is disagreement north of 30°N during winter and spring, when simulations predict a strong increase around 30°N. The AIRS retrievals do not show such an increase. When comparing signatures over oceans versus land, the discrepancy is larger for ocean regions in the Northern Hemisphere, while it is larger for land regions in the Southern Hemisphere. The ocean-land separation reveals that AIRS retrievals are quite different over land compared to the oceans in the extratropics. Furthermore, the temporal variance of AIRS retrievals over land is generally substantially larger than over the oceans, a feature that is not expected from atmospheric transport considerations alone.

[24] We also compared the simulated and retrieved spatial patterns for the four seasons separately (Figures 10a and 10b). The retrieved CO_2 fields have more fine scale spatial structure and are much less zonally symmetrical than the model simulations. During the first half of the year, the simulations exhibit a north-south gradient in the Northern Hemisphere, but the retrievals do not exhibit such a gradient. The gradient predicted by TM3 is somewhat larger than predicted by LMDZ, indicating that LMDZ is more diffusive than TM3.

[25] There are also some specific features in the retrievals that are suspicious at first sight. During the first 8 months of the year, there is an elevation in CO_2 concentrations over North America that is not shown by the model simulations. Elevated CO_2 values are also seen to the west of Africa during May to June 2003, which is reminiscent of dust

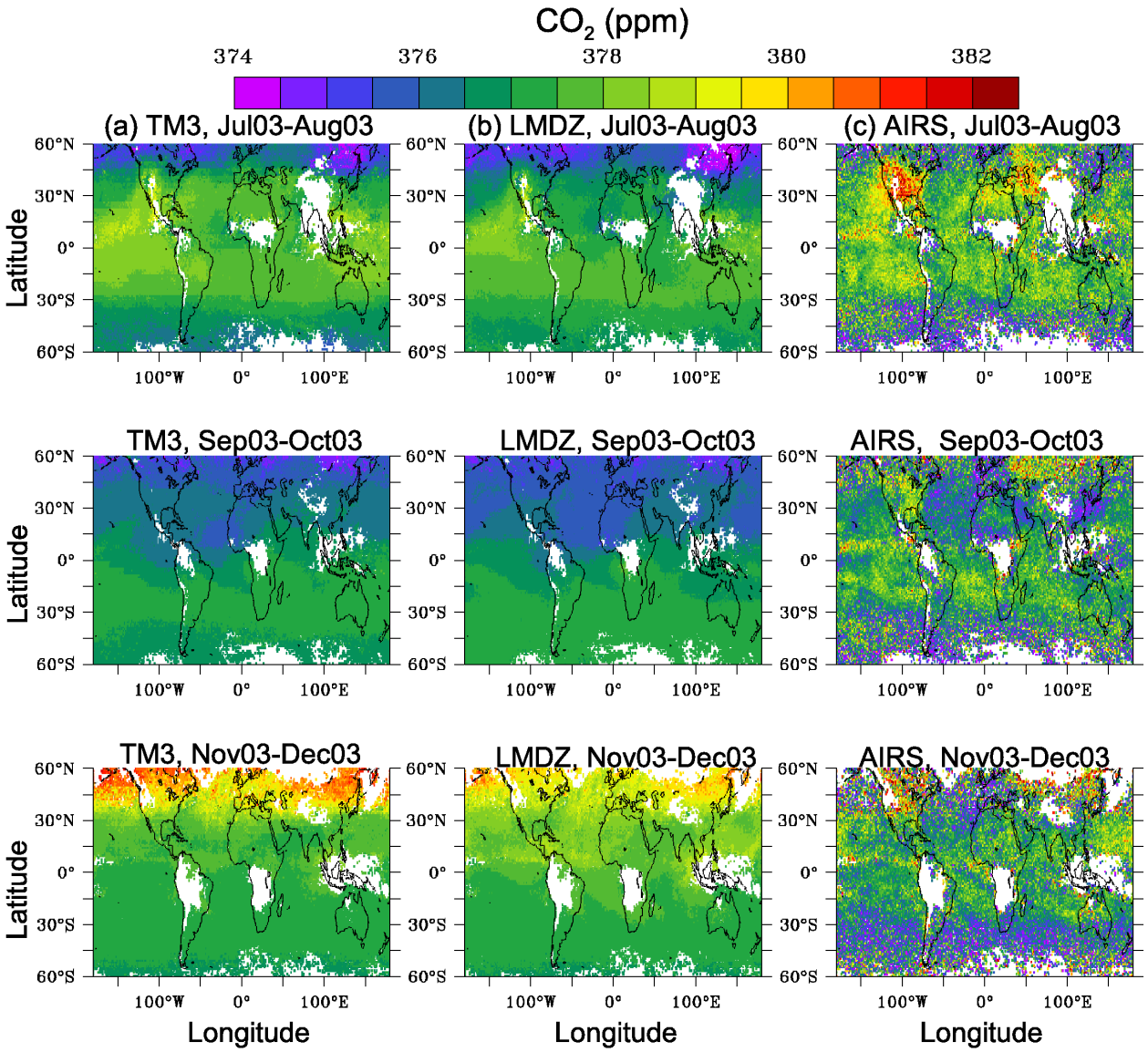

Figure 10b. Same as Figure 10a, but for the second half of the year 2003.

blown from the Sahara to the tropical Atlantic. As already pointed out earlier, this increased CO_2 can either be due to biomass burning, or to an adverse effect of aerosol scattering on the CO_2 estimation. Extensive study of the retrievals in these areas did not reveal any obvious error sources. Further validation needs to be done, but little data for validation is available for these areas during 2003.

4. Summary and Outlook

[26] The comparisons presented here convey a somewhat mixed message regarding the use of CO_2 from AIRS observations for constraining carbon cycling. On the one hand, the good agreement of key large-scale signatures of atmospheric CO_2, like the seasonal cycle caused by the Northern Hemisphere land biosphere, or the decrease of the magnitude of this signal with latitude, is encouraging evidence that CO_2 from AIRS observations has the potential to reveal new aspects of the carbon cycle. The comparisons also indicate that model simulations using two different transport models using the same extrapolated surface fluxes agree more closely with one another than with the retrievals. This raises the possibility that modeled transport is similarly biased in both models. To test this possibility, it is necessary to confront model predictions of upper troposphere tracer concentrations with independent observations. This calls for upper troposphere transport tracer data like SF_6 and CO_2, which are currently sparse. At the same time, it forces us to investigate tracer transport from the planetary boundary layer to the upper troposphere in more detail. On the other hand, there are features in the retrievals that cannot be easily explained, and this clearly requires further investigation as well.

[27] CO_2 surface flux estimates based on inversions of atmospheric transport and atmospheric data are very sensitive to systematic errors in the data [*Gloor et al.*, 1999]. The sensitivity to data errors grows strongly with the decrease in the strength of the CO_2 signal, and thus with height above

ground. Because of the dilution of surface sources and sinks due to mixing in the troposphere, their signature is substantially degraded in the upper troposphere compared to the planetary boundary layer. As a consequence, surface fluxes estimated using upper troposphere CO_2 will be particularly sensitive to retrieval biases, and therefore any significant bias in the AIRS retrievals are deleterious to the quality of surface flux estimates. *Chevallier et al.* [2005] noticed that current individual AIRS retrievals have a much larger variability at any given latitude than the corresponding modeled concentrations, which may be caused by significant regional biases in the retrievals. We therefore conclude that CO_2 retrieved from space might eventually help to constrain carbon cycling, and help improve the modeling of transport in the mid and upper troposphere. However, further improvements in the retrievals in concert with independent evaluation of lower-to-upper troposphere transport modeling are a prerequisite.

[28] **Acknowledgments.** The work described in this paper was financially supported by the EC project COCO (EVG1-CT-2001-00056). Authors are very grateful to NOAA-CIRES Climate Diagnostics Center, Boulder, Colorado, who provided the NCEP reanalysis data from their web site at http://www.cdc.noaa.gov/. Discussions with Cyril Crevoisier helped to improve the manuscript. We also thank David Schimel, who helped initiate the project as coprincipal investigator on the COCO grant.

References

Andres, R. J., G. Marland, I. Fung, and E. Matthews (1996), A 1° × 1° distribution of carbon dioxide emissions from fossil fuel consumption and cement manufacture, 1950–1990, *Global Biogeochem. Cycles*, *10*, 419–429.

Aumann, H. H., et al. (2003), AIRS/AMSU/HSB on the Aqua mission: Design, science, objectives, data products and processing systems, *IEEE Trans. Geosci. Remote Sens.*, *41*, 253–264.

Aumann, H. H., D. Gregorich, and S. Gaiser (2005), AIRS hyper-spectral measurements for climate research: Carbon dioxide and nitrous oxide effects, *Geophys. Res. Lett.*, *32*, L12802, doi:10.1029/2005GL022564.

Bakwin, P. S., P. P. Tans, C. Zhao, W. Ussler, and E. Quesnell (1995), Measurements of carbon dioxide on very tall tower, *Tellus, Ser. B*, *47*, 535–549.

Boering, K. A., S. C. Wofsy, B. C. Daube, H. R. Schneider, M. Loewenstein, J. R. Podolske, and T. J. Conway (1996), Stratospheric mean ages and transport rates from observations of carbon dioxide and nitrous oxide, *Science*, *274*, 1340–1343.

Bousquet, P., P. Peylin, P. Ciais, C. Le Quere, P. Friedlingstein, and P. P. Tans (2000), Regional changes in carbon dioxide fluxes of land and oceans since 1980, *Science*, *290*, 1342–1346.

Bousquet, P., D. A. Hauglustaine, P. Peylin, C. Carouge, and P. Ciais (2005), Two decades of OH variability as infrared by an inversion of atmospheric transport and chemistry of methyl chloroform, *Atmos. Chem. Phys. Disc.*, *5*, 1679–1737.

Chedin, A., S. Serrar, R. Armante, N. A. Scott, and A. Hollingsworth (2002), Signatures of annual and seasonal variations of CO_2 and other greenhouse gases from NOAA/TOVS observations and model simulations, *J. Clim.*, *15*, 95–116.

Chedin, A., S. Serrar, N. A. Scott, C. Crevoisier, and R. Armante (2003), First global measurement of midtropospheric CO_2 from NOAA polar satellite, tropical zone, *J. Geophys. Res.*, *108*(D18), 4581, doi:10.1029/2003JD003439.

Chevallier, F., R. J. Engelen, and P. Peylin (2005), The contribution of AIRS data to the estimation of CO_2 sources and sinks, *Geophys. Res. Lett.*, *32*, L23801, doi:10.1029/2005GL024229.

Conway, T., P. P. Tans, L. S. Waterman, K. W. Thoning, D. Kitzis, K. Masarie, and N. Zhang (1994), Evidence for interannual variability of the carbon cycle from the national oceanic and atmospheric administration climate monitoring and diagnostics laboratory global air sampling network, *J. Geophys. Res.*, *99*, 22,831–22,855.

Crevoisier, C., A. Chedin, and N. A. Scott (2003), AIRS channel selection for CO_2 and other trace gas retrievals, *Q. J. R. Meteorol. Soc.*, *129*, 2719–2740.

Crevoisier, C., S. Heilliette, A. Chédin, S. Serrar, R. Armante, and N. A. Scott (2004), Midtropospheric CO_2 concentration retrieval from AIRS observations in the tropics, *Geophys. Res. Lett.*, *31*, L17106, doi:10.1029/2004GL020141.

Engelen, R. J., and A. P. McNally (2005), Estimating atmospheric CO_2 from advanced infrared satellite radiances within an operational 4D-Var data assimilation system: Results and validation, *J. Geophys. Res.*, *110*, D18305, doi:10.1029/2005JD005982.

Engelen, R. J., E. Andersson, F. Chevallier, and A. Hollingsworth (2004), Estimating atmospheric CO_2 from advanced infrared satellite radiances within an operational 4D-Var data assimilation system: Methodology and first results, *J. Geophys. Res.*, *109*, D19309, doi:10.1029/2004JD004777.

Enting, I. G., C. M. Trudinger, and R. J. Francey (1995), A synthesis inversion of the concentration and δC^{13} of atmospheric CO_2, *Tellus, Ser. B*, *47*, 35–52.

Gloor, M., S.-M. Fan, S. W. Pacala, J. L. Sarmiento, and M. Ramonet (1999), A model-based evaluation of inversions of atmospheric transport, using annual mean mixing ratios, as a tool to monitor fluxes of nonreactive trace substances like CO_2 on a continental scale, *J. Geophys. Res.*, *104*, 14,245–14,260.

Gloor, M., S.-M. Fan, S. Pacala, and J. L. Sarmiento (2000), Optimal sampling of the atmosphere for purpose of inverse modeling: A model study, *Global Biogeochem. Cycles*, *14*, 407–428.

Gurney, K. R., et al. (2002), Towards robust regional estimates of CO_2 sources and sinks using atmospheric transport models, *Nature*, *415*, 626–630.

Heimann, M., and S. Körner (2003), *The Global Atmospheric Tracer Model TM3: Model Description and User's Manual Release 3.8a*, Max-Planck Inst. for Biogeochem., Jena, Germany.

Hourdin, F., and A. Armengaud (1999), Test of a hierarchy of finite-volume schemes for transport of trace species in an atmospheric general circulation model, *Mon. Weather Rev.*, *127*, 822–837.

Houweling, S., F.-M. Breon, I. Aben, C. Rödenbeck, M. Gloor, M. Heimann, and P. Ciais (2004), Inverse modeling of CO_2 sources and sinks using satellite data: A synthetic inter-comparison of measurement techniques and their performance as a function of space and time, *Atmos. Chem. Phys.*, *4*, 523–538.

Indermühle, A., B. Stauffer, and T. F. Stocker (1999), Early Holocene atmospheric CO_2 concentrations, *Science*, *286*, 1815.

Intergovernmental Panel on Climate Change (2001), *Climate Change 2001: The Scientific Basis*, edited by J. T. Houghton et al., Cambridge Univ. Press, New York.

Kalnay, E., et al. (1996), The NCEP/NCAR 40-year reanalysis project, *Bull. Am. Meteorol. Soc.*, *77*, 437–471.

Keeling, C. D., S. C. Piper, and M. Heimann (1989), A three dimensional model of atmospheric CO_2 transport based on observed winds: 4, Mean annual gradients and interannual variations, in *Aspects of Climate Variability in the Pacific and the Western Americas*, *Geophys. Monogr. Ser.*, vol. 55, edited by D. H. Peterson, pp. 305–363, AGU, Washington, D. C.

Laval, K., R. Sadourny, and Y. Serafini (1981), Land surface processes in a simplified general circulation model, *Geophys. Astrophys. Fluid Dyn.*, *17*, 129–150.

Louis, J. F. (1979), A parametric model of vertical eddy fluxes in the atmosphere, *Boundary Layer Meteorol.*, *17*, 187–202.

Mahlman, J. D. (1997), Dynamics of transport processes in the upper troposphere, *Science*, *276*, 1079–1083.

Marland, G., R. M. Rotty, and N. L. Treat (1985), CO_2 from fossil fuel burning: Global distributions of emissions, *Tellus, Ser. B*, *37*, 243–258.

McNally, A. P., and P. D. Watts (2003), A cloud detection algorithm for high-spectral-resolution infrared sounders, *Q. J. R. Meteorol. Soc.*, *129*, 3411–3423.

Rayner, P. J., and D. M. O'Brien (2001), The utility of remotely sensed CO_2 concentration data in surface source inversions, *Geophys. Res. Lett.*, *28*, 175–178.

Rayner, P., I. Enting, R. Francey, and R. Langenfelds (1999), Reconstructing the recent carbon cycle from atmospheric CO_2, δCO_2 and O_2/N_2 observations, *Tellus, Ser. B*, *51*, 213–232.

Reichler, T., M. Dameris, and R. Sausen (2003), Determining the tropopause height from gridded data, *Geophys. Res. Lett.*, *30*(20), 2042, doi:10.1029/2003GL018240.

Rödenbeck, C. (2005), *Estimating CO_2* Sources and Sinks From Atmospheric Mixing Ratio Measurements Using a Global Inversion of Atmospheric Transport, *Tech. Rep. 6*, Max-Planck Inst. for Biogeochem., Jena, Germany.

Rödenbeck, C., S. Houweling, M. Gloor, and M. Heimann (2003), CO_2 flux history 1982–2001 inferred from atmospheric data using a global inversion of atmospheric tracer transport, *Atmos. Chem. Phys.*, *3*, 1919–1964.

Russell, G., and J. Lerner (1981), A new finite-differencing scheme for the tracer transport equation, *J. Appl. Meteorol.*, *20*, 1483–1498.

Sabine, C. L., et al. (2004), The oceanic sink for anthropogenic CO_2, *Science*, *305*, 367–371.

Sadourny, R., and K. Laval (1984), January and July performance of the LMD general circulation model, in *New Perspectives in Climate Modeling*, edited by A. Berger and C. Nicolis, pp. 173–198, Elsevier, New York.

Tans, P. P., I. Y. Fung, and T. Takahashi (1990), Observational constraints on the global atmospheric CO_2 budget, *Science*, *247*, 1431–1438.

Tiedtke, M. (1989), A comprehensive mass flux scheme for cumulus parameterization in large-scale models, *Mon. Weather Rev.*, *117*, 1179–1800.

B. H. Braswell, Institute for the Study of Earth Ocean and Space, University of New Hampshire, Morse Hall, 39 College Road, Durham, NH 03824-3525, USA. (rob.braswell@unh.edu)

F. Chevallier and P. Peylin, Laboratoire des Sciences du Climat et de l'Environnement, L'Orme des Merisiers, Bat 701, Point courrier 129, F-91191 Gif sur Yvette, France. (frederic.chevallier@cea.fr; philippe.peylin@cea.fr)

R. J. Engelen, Satellite Section, Research Department, European Centre for Medium-Range Weather Forecasts, Shinfield Park, Reading RG2 9AX, UK. (richard.engelen@ecmwf.int)

M. Gloor, Earth and Biosphere Institute and School of Geography, University of Leeds, Leeds LS2 9JT, UK. (e.gloor@leeds.ac.uk)

M. Heimann, S. Körner, C. Rödenbeck, and Y. K. Tiwari, Biogeochemical Systems, Max-Planck Institute for Biogeochemistry, Hans Knoell Strasse 10, D-07745 Jena, Germany. (martin.heimann@bgc-jena.mpg.de; stefan.koerner@bgc-jena.mpg.de; christian.roedenbeck@bgc-jena.mpg.de)